

## Crystal Structures and Solution Properties of Discrete Complexes Composed of Saddle-Distorted Molybdenum(V)-Dodecaphenylporphyrins and Keggin-Type Heteropolyoxometalates Linked by Direct Coordination

Atsutoshi Yokoyama,<sup>†</sup> Takahiko Kojima,<sup>\*,‡</sup> Kei Ohkubo,<sup>†</sup> and Shunichi Fukuzumi<sup>\*,†,§</sup>

<sup>†</sup>Department of Material and Life Science, Division of Advanced Science and Biotechnology, Graduate School of Engineering, Osaka University, Suita, Osaka 565-0871, Japan,

<sup>‡</sup>Department of Chemistry, Graduate School of Pure and Applied Sciences, University of Tsukuba, Tsukuba 305-8571, Japan, and <sup>§</sup>Department of Bioinspired Science, Ewha Womans University, Seoul 120-750, Korea

Received September 24, 2010

Reactions of a saddle-distorted Mo(V)-porphyrin complex, [Mo(DPP)(O)(H<sub>2</sub>O)]ClO<sub>4</sub> (1 · ClO<sub>4</sub>; DPP<sup>2-</sup> = dodecaphenylporphyrin dianion), with tetra-*n*-butylammonium (TBA) salts of Keggin-type heteropolyoxometalates (POMs), α-[XW<sub>12</sub>O<sub>40</sub>]<sup>n-</sup> (X=P, *n*=3; **2**; X=Si, *n*=4; **3**; X=B, *n*=5; **4**), in ethyl acetate/acetonitrile gave 2:1 complexes formulated as [{Mo(DPP)(O)}<sub>2</sub>(HPW<sub>12</sub>O<sub>40</sub>)] (**5**), [{Mo(DPP)(O)}<sub>2</sub>(H<sub>2</sub>SiW<sub>12</sub>O<sub>40</sub>)] (**6**), and [(*n*-butyl)<sub>4</sub>N]<sub>2</sub>[{Mo(DPP)(O)}<sub>2</sub>(HBW<sub>12</sub>O<sub>40</sub>)] (**7**) under mild reaction conditions. The crystal structures of the complexes were determined by X-ray crystallography. In these three complexes, named *Porphyrin Hamburgers*, the POM binds to two Mo(V) centers of porphyrin units directly via coordination of two terminal oxo groups. In spite of the similarity of those POM's structures, those *Porphyrin Hamburgers* exhibit different coordination bond angles between POM and the Mo(V) center in the porphyrin: **5** and **7** show two different coordination bond angles in one molecule in contrast to **6**, which exhibits only one coordination bond angle. The *Porphyrin Hamburgers* involve protonation of the POM moieties to adjust the charge balance, as confirmed by spectroscopic titration with bases. In the crystals, the *Porphyrin Hamburgers* form two-dimensional (2D) sheets in the *ac* plane based on π–π interactions among peripheral phenyl substituents. Stacking of the 2D sheets toward the *b* axis constructs a 3D layered structure involving channels running into the crystallographic [1 0 0] and [0 0 1] directions in the crystal to include solvent molecules of crystallization for **5**–**7**, and also counter cations for **7**. Three complexes were revealed to be stable enough to maintain their structures even in solutions to show molecular ion peaks in the MALDI-TOF-MS measurements. They also exhibited different electron paramagnetic resonance (EPR) signals because of the Mo(V) (*S*=1/2, *l*=0) centers, reflecting the difference in the crystal structures. In addition, these complexes showed reversible multistep redox processes as observed in their cyclic voltammograms in benzonitrile to demonstrate high stability throughout the redox reactions in solution.

### Introduction

Porphyrins and their metal complexes have been known as useful materials for construction of supramolecular structures because of their rigid planar structures.<sup>1,2</sup> From the viewpoint of building blocks for supramolecules, metal-porphyrins have been widely used to construct robust

three-dimensional (3D) frameworks in the crystal because of facile synthetic methodology and manipulation of electronic characteristics and properties by introducing various functional groups.<sup>3–6</sup> Introduction of substituents to the *meso*-positions of porphyrin and the β-positions of pyrroles

\*To whom correspondence should be addressed. E-mail: kojima@chem.tsukuba.ac.jp (T.K.), fukuzumi@chem.eng.osaka-u.ac.jp (S.F.).

(1) (a) Drain, C. M.; Varotto, A.; Radivojevic, I. *Chem. Rev.* **2009**, *109*, 1630. (b) D'Souza, F.; Ito, O. *Chem. Commun.* **2009**, 4913. (c) Tashiro, K.; Aida, T. *Chem. Soc. Rev.* **2007**, *36*, 189. (d) Satake, A.; Kobuke, Y. *Org. Biomol. Chem.* **2007**, *5*, 1679. (e) Scandola, F.; Chiorboli, C.; Prodi, A.; Ingo, E.; Alessio, E. *Coord. Chem. Rev.* **2006**, *250*, 1471. (f) D'Souza, F.; Ito, O. *Coord. Chem. Rev.* **2005**, *74*, 765.

(2) (a) Fukuzumi, S.; Honda, T.; Ohkubo, K.; Kojima, T. *Dalton Trans.* **2009**, 3880. (b) Fukuzumi, S.; Kojima, T. *J. Mater. Chem.* **2008**, *18*, 1427. (c) Fukuzumi, S. In *Functional Organic Materials*; Müller, T. J., Bunz, U. H. F., Eds.; Wiley-VCH: Weinheim; 2008; pp 465–510.

(3) (a) Cuesta, L.; Karnas, E.; Lynch, V. M.; Chen, P.; Shen, J.; Kadish, K. M.; Ohkubo, K.; Fukuzumi, S.; Sessler, J. L. *J. Am. Chem. Soc.* **2009**, *131*, 13538. (b) Sessler, J. L.; Karnas, E.; Kim, S. K.; Ou, Z.; Zhang, M.; Kadish, K. M.; Ohkubo, K.; Fukuzumi, S. *J. Am. Chem. Soc.* **2008**, *130*, 15256.

(4) (a) Yamaguchi, S.; Shinokubo, H.; Osuka, A. *J. Am. Chem. Soc.* **2010**, *132*, 9992. (b) Yamaguchi, S.; Katoh, T.; Shinokubo, H.; Osuka, A. *J. Am. Chem. Soc.* **2008**, *130*, 14440. (c) Kamada, T.; Aratani, N.; Ikeda, T.; Shibata, N.; Higuchi, Y.; Wakamiya, A.; Yamaguchi, S.; Kim, K. S.; Yoon, Z. S.; Kim, D.; Osuka, A. *J. Am. Chem. Soc.* **2006**, *128*, 7670.

(5) (a) Kelley, R. F.; Lee, S. J.; Wilson, T. M.; Nakamura, Y.; Tiede, D. M.; Osuka, A.; Hupp, J. T.; Wasielewski, M. R. *J. Am. Chem. Soc.* **2008**, *130*, 4277. (b) Kelley, R. F.; Shin, W. S.; Rybtchinski, B.; Sinks, L. E.; Wasielewski, M. R. *J. Am. Chem. Soc.* **2007**, *129*, 3173.

makes it possible to utilize them as building blocks having functional groups for hydrogen bonding,<sup>7</sup>  $\pi$ - $\pi$  interactions<sup>8</sup> and coordination,<sup>9</sup> to connect each component toward the emergence of novel structural motifs, which are unique for porphyrins and metalloporphyrins. Coordination bonds of peripheral functional groups to metal centers in adjacent metalloporphyrins can give rise to the formation of 3D lattice frameworks.<sup>10</sup> As for such coordination polymers containing metalloporphyrins, they can be applied not only to the formation of 3D frameworks but also to the construction of functional materials based on their excellent photochemical and redox properties.<sup>6,11</sup>

On the other hand, heteropolyoxometalate or polyoxometalates (POMs) and their derivatives have attracted particular attention<sup>12</sup> in terms of their specific functions: catalyzing oxidation reactions,<sup>13</sup> multiple-redox processes,<sup>14</sup> energy transfer by the ultraviolet irradiation.<sup>15</sup> In general, POMs can dissolve into only polar solvents including water. POMs are colorless, absorbing no visible light. To explore further application of purely inorganic POMs, it should be useful and desirable to establish a strategy to functionalize POMs with organic or organometallic functional molecules. This may improve solubility into less polar solvents and give new functionality based on visible light absorption toward the development of POM-based functional molecules.

Since POMs have terminal oxo and bridging oxo groups to form hydrogen bonding, formation of supramolecular structures has been demonstrated and applied to create functional materials,<sup>16,17</sup> including to adsorb molecular entities.<sup>18</sup> In particular, the coordination of POMs to metal ions has been a challenge to construct well-organized discrete structures as a molecule toward the development of POM-containing functional molecules and thereby functional materials as their assemblies: the construction of molecular complexes involving POMs has been recognized to be extremely difficult because of the strong acidity of the POMs. Thus, severe reaction conditions such as hydrothermal methods<sup>19</sup> or strongly Lewis-acidic metal ions, such as lanthanides,<sup>20</sup> have been required to synthesize such assemblies of inorganic-organic hybrid materials based on metal complexes with organic ligands. Although Zubietta and co-workers have demonstrated formation of metalloporphyrin-POM assemblies by hydrothermal methods, no direct interaction has been recognized between those two components in the crystal structure, but forming only ion pairs without direct bonding interactions.<sup>21</sup> Some porphyrin-POM assemblies have been synthesized without using hydrothermal methods, however, those complexes have been prepared as films<sup>22</sup> or precipitates<sup>23</sup> without clarifying their molecular structures and intermolecular interactions. Thus, toward construction of functional complexes made of metalloporphyrins and POMs, a reasonable synthetic methodology needs to be established under mild reaction conditions to regulate the reactions in a well-defined manner.

Recently, we have reported on enhanced Lewis acidity of the metal center coordinated by a saddle-distorted porphyrin compared with that coordinated by a planar porphyrin.<sup>24</sup> To construct metalloporphyrin-POM complexes, the strong Lewis acidity of the metal center coordinated by a saddle-distorted porphyrin can be expected to provide intensive interactions with Lewis basic POMs to stabilize the complexes based on the axial coordination to the metal center of a positively charged metal-porphyrin complex. Thus, we examined the reaction of saddle-distorted  $[\text{Mo}^{\text{V}}(\text{DPP})(\text{O})(\text{H}_2\text{O})]^+$

- (6) (a) D'Souza, F.; Subbaiyan, N. K.; Xie, Y.; Hill, J. P.; Ariga, K.; Ohkubo, K.; Fukuzumi, S. *J. Am. Chem. Soc.* **2009**, *131*, 16138. (b) D'Souza, F.; Maligaspe, E.; Ohkubo, K.; Zandler, M. E.; Subbaiyan, N. K.; Fukuzumi, S. *J. Am. Chem. Soc.* **2009**, *131*, 8787. (c) Takai, A.; Chkounda, M.; Eggenspieler, A.; Gros, C. P.; Lachkar, M.; Barbe, J.-M.; Fukuzumi, S. *J. Am. Chem. Soc.* **2010**, *132*, 4477. (d) D'Souza, F.; Smith, P. M.; Zandler, M. E.; McCarty, A. L.; Ito, M.; Araki, Y.; Ito, O. *J. Am. Chem. Soc.* **2004**, *126*, 7898.
- (7) (a) Shi, X.; Barkigia, K. M.; Fajer, J.; Drain, C. M. *J. Org. Chem.* **2001**, *66*, 6513. (b) Diskin-Posner, Y.; Goldberg, I. *Chem. Commun.* **1999**, 1961. (c) Goldberg, I. *Chem. Commun.* **2005**, 1243. (d) Lipstman, S.; Muniappan, S.; Goldberg, I. *Acta Crystallogr.* **2007**, *C63*, m300-o395.
- (8) (a) Shirakawa, M.; Fujita, N.; Shinkai, S. *J. Am. Chem. Soc.* **2005**, *127*, 4164. (b) Yuasa, M.; Oyaizu, K.; Yamaguchi, A.; Kuwakado, M. *J. Am. Chem. Soc.* **2004**, *126*, 11128. (c) Wang, Z.; Medforth, C. J.; Shelnutt, J. A. *J. Am. Chem. Soc.* **2004**, *126*, 15954. Saltsman, I.; Goldberg, I.; Balasz, Y.; Gross, Z. *Tetrahedron Lett.* **2007**, *48*, 239. (d) Saltsman, I.; Goldberg, I.; Balasz, Y.; Gross, Z. *Tetrahedron Lett.* **2007**, *48*, 239.
- (9) (a) Abrahams, B. F.; Hoskins, B. F.; Michail, D. M.; Robson, R. *Nature* **1994**, *369*, 727. (b) Kobuke, Y.; Ogawa, K. *Bull. Chem. Soc. Jpn.* **2003**, *76*, 689. (c) Shoji, O.; Tanaka, H.; Kawai, T.; Kobuke, Y. *J. Am. Chem. Soc.* **2005**, *127*, 8598. (d) Drain, C. M.; Nifftatis, F.; Vasenko, A.; Batteas, J. D. *Angew. Chem., Int. Ed.* **1998**, *37*, 2344. (e) Milic, T. N.; Chi, N.; Yablon, D. G.; Flynn, G. W.; Batteas, J. D.; Drain, C. M. *Angew. Chem., Int. Ed.* **2002**, *41*, 2117. (f) Diskin-Posner, Y.; Dahal, S.; Goldberg, I. *Angew. Chem., Int. Ed.* **2000**, *39*, 1288. (g) Muniappan, S.; Lipstman, S.; George, S.; Goldberg, I. *Angew. Chem.* **2007**, *46*, 5544. (h) Falber, A.; Todaro, L.; Goldberg, I.; Favilla, M. V.; Drain, C. M. *Inorg. Chem.* **2008**, *47*, 454.
- (10) (a) Kosal, M. E.; Chou, J.-H.; Wilson, S. R.; Suslick, K. S. *Nat. Mater.* **2002**, *1*, 118. (b) Suslick, K. S.; Bhyrappa, P.; Chou, J.-H.; Kosal, M. E.; Nakagaki, S.; Smitherly, D. W.; Wilson, S. R. *Acc. Chem. Res.* **2005**, *38*, 283.
- (11) (a) Kumar, R. K.; Goldberg, I. *Angew. Chem., Int. Ed.* **1998**, *37*, 3027. (b) Goldberg, I. *Chem.—Eur. J.* **2000**, *6*, 3863.
- (12) Katsoulis, D. E. *Chem. Rev.* **1998**, *98*, 359.
- (13) (a) Kozhevnikov, I. V. *Chem. Rev.* **1998**, *98*, 171. (b) Neumann, R.; Dahani, M. *J. Am. Chem. Soc.* **1998**, *120*, 11969. (c) Neumann, R.; Khenkin, A. M. *Inorg. Chem.* **1995**, *34*, 5753. (d) Azizi, N.; Torkiyani, L.; Saidi, M. R. *Org. Lett.* **2006**, *8*, 2079. (e) Kamata, K.; Yonehara, K.; Sumida, Y.; Yamaguchi, K.; Hikichi, S.; Mizuno, N. *Science* **2003**, *300*, 964. (f) Nakazawa, Y.; Kamata, K.; Kotani, M.; Yamaguchi, K.; Mizuno, N. *Angew. Chem., Int. Ed.* **2005**, *44*, 5136. (g) Bareyt, S.; Piligkos, S.; Hasenknopf, B.; Gouzerh, P.; Lacôte, E.; Thorimbert, S.; Malacria, M. *J. Am. Chem. Soc.* **2005**, *127*, 6788.
- (14) (a) Zhang, J.; Bond, A. M.; MacFarlane, D. R.; Forsyth, S. W.; Pringle, J. M.; Mariotti, A. W. A.; Glowinski, A. F.; Wedd, A. G. *Inorg. Chem.* **2005**, *44*, 5123. (b) Sadakane, M.; Steckhan, E. *Chem. Rev.* **1998**, *98*, 219.
- (15) Yamase, T. *Chem. Rev.* **1998**, *98*, 307.

- (16) (a) Harada, R.; Mastuda, Y.; Okawa, H.; Kojima, T. *Angew. Chem., Int. Ed.* **2004**, *43*, 1825. (b) Kojima, T.; Harada, R.; Nakanishi, T.; Kaneko, K.; Fukuzumi, S. *Chem. Mater.* **2007**, *19*, 51.

- (17) (a) Fang, X.; Kogerler, P.; Isaacs, L.; Uchida, S.; Mizuno, N. *J. Am. Chem. Soc.* **2009**, *131*, 432. (b) Akutagawa, T.; Endo, D.; Noro, S.-I.; Cronin, L.; Nakamura, T. *Coord. Chem. Rev.* **2007**, *251*, 2547. (c) Akutagawa, T.; Endo, D.; Kudo, F.; Noro, S.-I.; Takeda, S.; Cronin, L.; Nakamura, T. *Cryst. Growth Des.* **2008**, *8*, 812. (d) Chatterjee, T.; Sarma, M.; Das, S. K. *Cryst. Growth Des.* **2010**, *10*, 3149.

- (18) (a) Ishii, Y.; Takenaka, Y.; Konishi, K. *Angew. Chem., Int. Ed.* **2004**, *43*, 2702. (b) Ishii, Y.; Nakayama, N.; Konishi, K. *Chem. Lett.* **2007**, *36*, 246.

- (19) (a) Tain, A. X.; Ying, J.; Peng, J.; Sha, J. Q.; Pang, H. J.; Zhang, P. P.; Chen, Y.; Zhu, M.; Su, Z. M. *Inorg. Chem.* **2009**, *48*, 100. (b) Tain, A. X.; Ying, J.; Peng, J.; Sha, J. Q.; Su, Z. M.; Pang, H. J.; Zhang, P. P.; Chen, Y.; Zhu, M.; Shen, Y. *Cryst. Growth Des.* **2010**, *10*, 1104. (c) Li, G.; Salim, C.; Hinode, H. *Solid State Sci.* **2008**, *10*, 121. (d) Lu, Y.; Li, Y.; Wang, E.; Lü, J.; Xu, L.; Clérac, R. *Eur. J. Inorg. Chem.* **2005**, 1239.

- (20) (a) An, H.; Xial, D.; Wang, E.; Sun, C.; Xu, L. *J. Mol. Struct.* **2005**, *743*, 117. (b) Falber, A.; Burton-Pye, B. P.; Radivojevic, I.; Todaro, L.; Saleh, R.; Francesconi, L. C.; Drain, C. M. *Eur. J. Inorg. Chem.* **2009**, 2459.

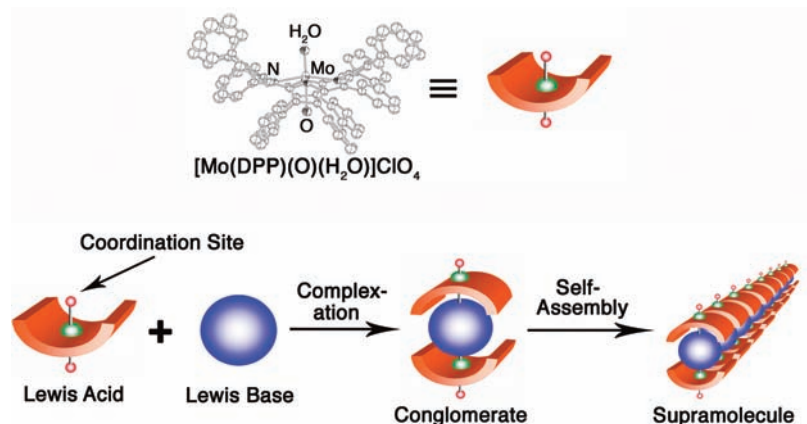
- (21) Hagrman, D.; Hagrman, P. J.; Zubietta, J. *Angew. Chem., Int. Ed.* **1999**, *38*, 3165.

- (22) Bazzan, G.; Smith, W.; Francesconi, L. C.; Drain, C. M. *Langmuir* **2008**, *24*, 3244.

- (23) Santos, I. C. M. S.; Rebelo, S. L. H.; Balula, M. S. S.; Martins, R. R. L.; Pereira, M. M. M. S.; Simões, M. M. Q.; Neves, M. G. P. M. S.; Cavaleiro, J. A. S.; Cavaleiro, A. M. V. *J. Mol. Catal. A: Chem.* **2005**, *231*, 35.

- (24) Kojima, T.; Nakanishi, T.; Honda, T.; Harada, R.; Shiro, M.; Fukuzumi, S. *Eur. J. Inorg. Chem.* **2009**, 727.

Scheme 1



(DPP = dodecaphenylporphyrinato) with well-defined and stable Keggin-type POMs, which can be regulated in sizes, shapes, and charges to construct discrete and stable complexes having well-controlled structures, consisting of those two units linked by strong coordination bonds. Therefore, we adopted three kinds of Keggin-type POMs ( $\alpha$ -[PW<sub>12</sub>O<sub>40</sub>]<sup>3-</sup> (**2**),  $\alpha$ -[SiW<sub>12</sub>O<sub>40</sub>]<sup>4-</sup> (**3**),  $\alpha$ -[BW<sub>12</sub>O<sub>40</sub>]<sup>5-</sup> (**4**))<sup>25</sup> as Lewis-basic reactants toward [Mo<sup>V</sup>(DPP)(O)(H<sub>2</sub>O)]<sup>+</sup> to prepare stable and discrete complexes and also supramolecular assemblies on the basis of strong axial coordination of the POMs as described in Scheme 1.

We report herein the syntheses, crystal structures, and solution properties of novel discrete and nanosized metalloporphyrin-POM complexes having direct bonding between those two species. Those are discrete nanosized molecular complexes, formulated as [{Mo(DPP)(O)}<sub>2</sub>(HPW<sub>12</sub>O<sub>40</sub>)] (**5**), [{Mo(DPP)(O)}<sub>2</sub>(H<sub>2</sub>SiW<sub>12</sub>O<sub>40</sub>)] (**6**),<sup>26</sup> and TBA<sub>2</sub>[{Mo(DPP)(O)}<sub>2</sub>(HBW<sub>12</sub>O<sub>40</sub>)] (**7**) (TBA = tetra(*n*-butyl)ammonium ion). In these three molecules, two [Mo(DPP)(O)]<sup>+</sup> units directly bind to one Keggin-type POM via the coordination of two terminal oxo groups of the POM.

## Experimental Section

**General Procedures.** All chemicals available were purchased from appropriate commercial sources and used as received without further purification unless otherwise noted. Benzotrile (PhCN) was distilled from P<sub>2</sub>O<sub>5</sub> and stored over 4 Å molecular sieves. Dichloromethane (CH<sub>2</sub>Cl<sub>2</sub>) and acetonitrile (CH<sub>3</sub>CN) was distilled from CaH<sub>2</sub> under N<sub>2</sub> just prior to use. All other solvents were special grade and were used as received from commercial sources without further purification. Column chromatography was performed on a silica gel Waco-gel C-200 (60–200 mesh) or activated alumina (ca. 200 mesh), both from Waco Pure Chemicals. UV–vis spectroscopy was carried out on a JASCO V-570 UV/vis/NIR spectrometer at room temperature. MALDI-TOF-MS spectra were recorded on a Shimadzu Kratos Compact MALDI I for **5** and **7** and a Bruker Daltonics ultrafleXtreme spectrometer for **6**, using  $\alpha$ -cyano-4-hydroxycinnamic acid (CHCA) as a matrix. The ESI-MS spectrum was recorded on API-300 triple-quadrupole mass spectrometer (PE-Sciex). XPS spectra were obtained by using a PHYSICAL ELECTRONICS  $\phi$  5800 ESCA. Cyclic voltammograms and differential pulse voltammograms were obtained on an ALS/[H] CH Instruments Electrochemical Analyzer Model 630B in

benzonitrile as solvent at room temperature in the presence of TBAPF<sub>6</sub> as an electrolyte under Ar (scan rate: 100 mV/s). Elemental analysis data for Organic Compounds, Department of Chemistry, Kyushu University and Department of Material and Life Science, Osaka University.

**Safety Note. Caution!** Perchlorate salts of metal complexes with organic ligands are potentially explosive. They should be handled with great care in small quantities.

**Synthesis.** H<sub>2</sub>DPP,<sup>27</sup> [Mo(DPP)(O)(OCH<sub>3</sub>)],<sup>24</sup>  $\alpha$ -K<sub>4</sub>[SiW<sub>12</sub>O<sub>40</sub>] $\cdot$ 17H<sub>2</sub>O,<sup>25</sup> and  $\alpha$ -K<sub>5</sub>[BW<sub>12</sub>O<sub>40</sub>] $\cdot$ xH<sub>2</sub>O<sup>28</sup> were prepared according to the literature methods.

[Mo(DPP)(O)(H<sub>2</sub>O)]ClO<sub>4</sub> (**1**  $\cdot$  ClO<sub>4</sub>). [Mo(DPP)(O)(OCH<sub>3</sub>)] (781 mg, 0.572 mmol) was dissolved in 200 mL of CH<sub>2</sub>Cl<sub>2</sub>, and the resulting solution was washed with three 100 mL portions of 2% aqueous HClO<sub>4</sub> in a separatory funnel.<sup>29</sup> The resulting CH<sub>2</sub>Cl<sub>2</sub> solution was dried with MgSO<sub>4</sub>, filtered, and concentrated to 5 mL under reduced pressure. The remaining solution was layered with hexane. Green crystals (712 mg, 92.1%) were obtained after 1 week. Anal. Calcd for C<sub>92</sub>H<sub>62</sub>ClMoN<sub>4</sub>O<sub>6</sub>: C 76.16, H 4.31, N 3.86. Found: C 76.13, H 4.73, N 3.77.

$\alpha$ -[(*n*-C<sub>4</sub>H<sub>9</sub>)<sub>4</sub>N]<sub>3</sub>[PW<sub>12</sub>O<sub>40</sub>] (**2**).  $\alpha$ -Na<sub>3</sub>PW<sub>12</sub>O<sub>40</sub> was obtained from a commercial source and used without further purification. A solution of  $\alpha$ -Na<sub>3</sub>[PW<sub>12</sub>O<sub>40</sub>] (5.00 g, 1.70 mmol) in 10 mL of water was added to 10 mL of aqueous solution of TBABr (2.50 g, 7.76 mmol). White precipitate formed was filtered, washed with a large amount of water, and dissolved into 10 mL of CH<sub>3</sub>CN. A large amount of water was added to the solution, then the white precipitate was filtered, and dried under vacuum (4.50 g, 73.5%). Anal. Calcd for C<sub>48</sub>H<sub>108</sub>N<sub>3</sub>O<sub>40</sub>PW<sub>12</sub>: C 16.00, H 3.02, N 1.17; found: C 16.00, H 3.01, N 1.19.

$\alpha$ -[(*n*-C<sub>4</sub>H<sub>9</sub>)<sub>4</sub>N]<sub>4</sub>[SiW<sub>12</sub>O<sub>40</sub>] (**3**) and  $\alpha$ -[(*n*-C<sub>4</sub>H<sub>9</sub>)<sub>4</sub>N]<sub>5</sub>[BW<sub>12</sub>O<sub>40</sub>] (**4**). A similar method was applied to prepare these compounds by using  $\alpha$ -K<sub>4</sub>[SiW<sub>12</sub>O<sub>40</sub>] $\cdot$ 17H<sub>2</sub>O (5.13 g, 1.54 mmol) for **3** and  $\alpha$ -K<sub>5</sub>[BW<sub>12</sub>O<sub>40</sub>] $\cdot$ xH<sub>2</sub>O (5.50 g, 1.80 mmol) for **4**. Yield: 4.41 g, 74.0% for **3**; 4.48 g, 61.1% for **4**. Anal. Calcd for C<sub>64</sub>H<sub>114</sub>N<sub>4</sub>O<sub>40</sub>-SiW<sub>12</sub> (**3**): C 20.00, H 3.78, N 1.46; found: C 19.99, H 3.76, N 1.46; calcd for C<sub>80</sub>H<sub>180</sub>N<sub>5</sub>O<sub>40</sub>BW<sub>12</sub> (**4**): C 23.61, H 4.46, N 1.72; found: C 23.43, H 4.18, N 1.66.

[[Mo(DPP)(O)]<sub>2</sub>(HPW<sub>12</sub>O<sub>40</sub>)] (**5**). [Mo(DPP)(O)(H<sub>2</sub>O)]ClO<sub>4</sub> (100 mg, 0.069 mmol) in 10 mL of CH<sub>2</sub>Cl<sub>2</sub> was mixed with **2** (110 mg, 0.031 mmol) dissolved in 10 mL of CH<sub>3</sub>CN. The solution was heated at 40 °C for 2 h and evaporated to dryness. The resulting

(27) (a) Medforth, C. J.; Senge, M. O.; Smith, K. M.; Sperks, L. D.; Shelnutt, J. A. *J. Am. Chem. Soc.* **1992**, *114*, 9859. (b) Liu, C.-J.; Yu, W.-Y.; Peng, S.-M.; Mak, T. C. W.; Che, C.-M. *J. Chem. Soc., Dalton Trans.* **1998**, 1805.

(28) Rocchiccioli-Deltcheff, C.; Fournier, M.; Franck, R.; Thouvenot, R. *Inorg. Chem.* **1983**, *42*, 207.

(29) Hamstra, B. J.; Cheng, B.; Ellison, M. K.; Scheidt, W. R. *Inorg. Chem.* **1999**, *38*, 3554.

(25) Tézé, A.; Hervé, G. *Inorg. Synth.* **1990**, *27*, 93.

(26) For a preliminary report on **6** see: Yokoyama, A.; Kojima, T.; Ohkubo, K.; Fukuzumi, S. *Chem. Commun.* **2007**, 3997.

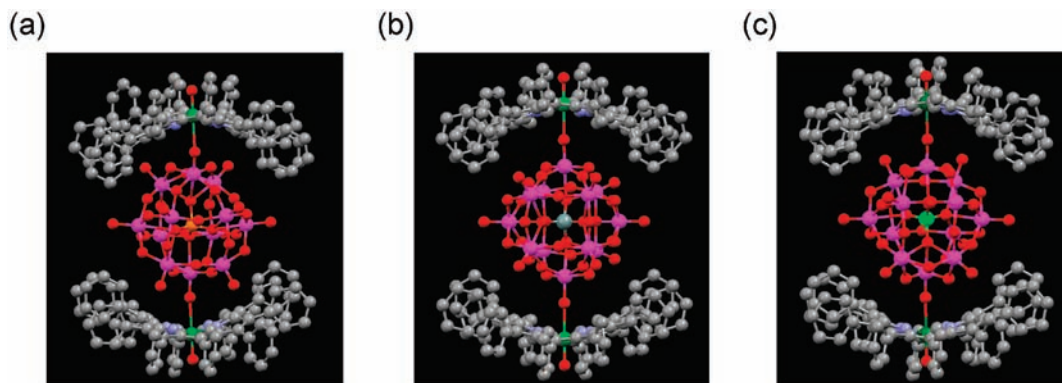


**Figure 1.** Crystal Structures of **5** (a), **6** (b), and the anion moiety of **7** (c). Gray, carbon; blue, nitrogen; red, oxygen; green, molybdenum; pink, tungsten; orange, phosphorus; dark gray, silicon; light green, boron.

brown powder was dissolved in  $\text{CH}_2\text{Cl}_2/\text{CH}_3\text{CN}$ , and the diffusion of hexane vapor into the solution for 4 days gave brown crystals of **5** (25.4 mg). MALDI-TOF-MS (negative mode): 5543.94 (observed,  $[\text{M} - \text{H}]^-$ ); 5544.55 (calcd for  $[\text{C}_{184}\text{H}_{120}\text{N}_8\text{O}_{42}\text{PMo}_2\text{W}_{12}]^-$ ). A single crystal suitable for X-ray crystallography was obtained by recrystallization from the same solvent system at room temperature.

$\{[\text{Mo}(\text{DPP})(\text{O})]_2(\text{H}_2\text{SiW}_{12}\text{O}_{40})\}$  (**6**).  $[\text{Mo}(\text{DPP})(\text{O})(\text{H}_2\text{O})]\text{ClO}_4$  (100 mg, 0.069 mmol) in 10 mL of  $\text{CH}_3\text{C}(\text{O})\text{OC}_2\text{H}_5$  (AcOEt) was mixed with **3** (103 mg, 0.027 mmol) dissolved in 10 mL of  $\text{CH}_3\text{CN}$ . The diffusion of hexane vapor into the solution for 4 days gave brown crystals of **6** (31.2 mg). MALDI-TOF-MS (negative mode): 5542.10 (observed,  $[\text{M} - \text{H}]^-$ ); 5542.00 (calcd for  $[\text{C}_{184}\text{H}_{121}\text{N}_8\text{O}_{42}\text{SiMo}_2\text{W}_{12}]^-$ ). A single crystal suitable for X-ray crystallography was obtained by recrystallization from the same solvent system at  $0^\circ\text{C}$ .

$\{(n\text{-C}_4\text{H}_9)_4\text{N}\}_2\{[\text{Mo}(\text{DPP})(\text{O})]_2(\text{HBW}_{12}\text{O}_{40})\}$  (**7**).  $[\text{Mo}(\text{DPP})(\text{O})(\text{H}_2\text{O})]\text{ClO}_4$  (100 mg, 0.069 mmol) in 10 mL of AcOEt was mixed with **4** (120 mg, 0.031 mmol) dissolved in 10 mL of  $\text{CH}_3\text{CN}$ . The diffusion of hexane vapor into the solution for 7 days gave brown crystals of **7** (50.2 mg). MALDI-TOF-MS (negative mode): 5525.79 (observed,  $[\text{M} + \text{H} - 2\text{TBA}]^-$ ); 5526.36 (calcd for  $[\text{C}_{184}\text{H}_{122}\text{N}_8\text{O}_{42}\text{BMo}_2\text{W}_{12}]^-$ ). The sample was dried in vacuo at  $150^\circ\text{C}$  for 6 h and then submitted to elemental analysis. Anal. Calcd for  $\text{C}_{216}\text{H}_{193}\text{N}_{10}\text{O}_{42}\text{Mo}_2\text{BW}_{12}$ : C 43.17, H 3.24, N 2.33; found: C 43.08, H 3.54, N 2.48. A single crystal suitable for X-ray crystallography was obtained by recrystallization from the same solvent system at room temperature.

**Electrochemical Measurements.** Cyclic voltammograms (CV) and differential plus voltammograms (DPV) were obtained in PhCN in the presence of 0.1 M TBAPF<sub>6</sub> as an electrolyte under  $\text{N}_2$  at room temperature, with use of Pt electrode as a working electrode, Ag/AgNO<sub>3</sub> as a reference electrode, Pt wire as a auxiliary electrode. The values (vs Ag/AgNO<sub>3</sub>) were converted to those versus SCE by addition 0.29 V.

**Spectroscopic Titration of 5, 6, and 7.** UV-vis spectral titrations of **5** ( $1.0 \times 10^{-5}$  M), **6** ( $1.0 \times 10^{-5}$  M), and **7** ( $1.0 \times 10^{-5}$  M) upon adding base were measured in  $\text{CH}_2\text{Cl}_2$  and PhCN at room temperature. Triethylamine ( $\text{NEt}_3$ , 1 mM) and 1,8-bis(dimethylamino)naphthalene (proton sponge, 3 mM) were used as bases.

**EPR Measurements.** Electron paramagnetic resonance (EPR) spectra were recorded on a JEOL JEX-REIXE spectrometer, and  $g$  values were determined using an  $\text{Mn}^{2+}$  marker in  $\text{CH}_2\text{Cl}_2$  and PhCN at room temperature.

**X-ray Crystallography.** Single crystals of compounds were put in liquid paraffin and then were mounted on a glass fiber with silicon grease. All the diffraction data were collected on a Rigaku Mercury CCD diffractometer at  $-170 \pm 1$  (**1**) and  $-150 \pm 1$  (**5–7**)  $^\circ\text{C}$ . All calculations for structure refinements were carried out on a PC using the CrystalStructure (Rigaku

Corp., Japan)<sup>30</sup> and SHELXL programs.<sup>31</sup> Details of the X-ray analysis are described in the Supporting Information. In the structure refinements for **5** and **7**, we could not determine the positions of the solvent molecules of crystallization including water and acetonitrile molecules, which were clearly identified in difference Fourier maps, because of their severe disorder. Their contribution was thus subtracted from the diffraction pattern by the “Squeeze” program.<sup>32</sup> Crystallographic data for **6** has been available as CCDC-622714 from the Cambridge Crystallographic Data Centre.

## Results and Discussion

**Crystal Structure of  $[\text{Mo}(\text{DPP})(\text{O})(\text{H}_2\text{O})]\text{ClO}_4$ .** A Mo(V)-aqua complex,  $[\text{Mo}(\text{DPP})(\text{O})(\text{H}_2\text{O})]\text{ClO}_4$  (**1**·ClO<sub>4</sub>), was synthesized by exposing the solution of a precursor complex,  $[\text{Mo}(\text{DPP})(\text{O})(\text{OCH}_3)]$ , in  $\text{CH}_2\text{Cl}_2$  to 2% aqueous HClO<sub>4</sub> in a separatory funnel. The ligand substitution proceeded smoothly. Crystal structures of **1**·ClO<sub>4</sub> were depicted in Figure S1(a) (see Supporting Information); however, the severe disorder of three  $\text{CH}_2\text{Cl}_2$  molecules of crystallization did not allow us to discuss the details of its structure. The porphyrin macrocycle in **1** was confirmed to show saddle-distortion because of steric repulsion among peripheral phenyl groups.<sup>33</sup> Two  $[\text{Mo}(\text{DPP})(\text{O})(\text{H}_2\text{O})]\text{ClO}_4$  units are combined by hydrogen bonds between the aqua ligand and ClO<sub>4</sub><sup>−</sup> to form a supramolecular dimeric structure (see Figure S1(b) in Supporting Information).

**Crystal Structures of Porphyrin Hamburger Series.** The reaction of **1** with **2**, **3**, and **4** in  $\text{CH}_2\text{Cl}_2/\text{AcOEt}$  (for **5**) or  $\text{CH}_3\text{CN}/\text{AcOEt}$  (for **6** and **7**) followed by vapor diffusion of hexane gave brown-transparent crystals of discrete complexes **5**, **6**, and **7**, respectively. The reaction and crystallization occurred even in the dark, indicating that the formation of the complexes is not a photoinduced process. The crystal structures of **5**, **6**, and **7** were determined by X-ray crystallography. The crystal structures of **5**, **6**,<sup>26</sup> and **7** are shown in Figure 1. In these three crystal structures of the discrete complexes, named as *Porphyrin*

(30) CrystalStructure, Crystal Structure Analysis Package, 3.7.0; Rigaku and Rigaku/MS: The Woodlands, TX, 2000–2005.

(31) Sheldrick, G. M. *SIR 97 and SHELX 97, Program for Crystal Structures Refinement*; University of Göttingen: Göttingen, Germany, 1997.

(32) Sluis, P. V. D.; Spek, A. L. *Acta Crystallogr.* **1990**, *A46*, 194.

(33) Nurco, D. J.; Medforth, C. J.; Forsyth, T. P.; Olmstead, M. M.; Smith, K. M. *J. Am. Chem. Soc.* **1996**, *118*, 10918.

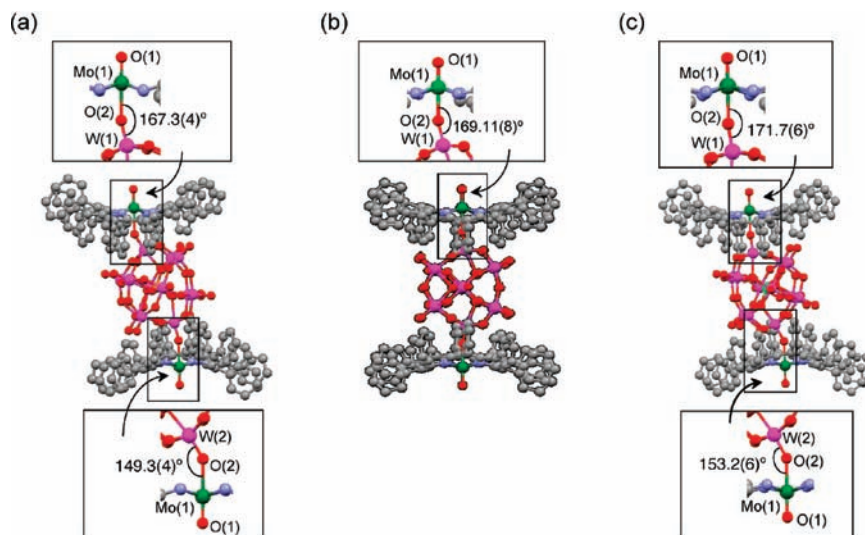


**Figure 2.** Coordination environments of Mo(V) centers in **5** (a), **6** (b), and **7** (c).

*Hamburgers*, the Mo<sup>V</sup> centers of two [Mo(DPP)(O)]<sup>+</sup> ions were bound directly to the terminal oxo groups of POMs. As for **5** and **7**, very large solvent-accessible voids can be found in their crystal structures, since the residual peaks of electron density for the disordered solvent molecules have been removed by the Squeeze method.<sup>32</sup>

The coordination of POMs occurs via ligand exchange of the aqua ligand to the POM during the recrystallization under mild reaction conditions to form a discrete and nanosized molecule (ca. 1.82 nm for the distance between the two oxo ligands of the [Mo(DPP)(O)]<sup>+</sup> units). Because of this direct coordination, the distortions of the DPP<sup>2-</sup> ligands are changed from saddle distortion to ruffling with saddle distortion because of the steric repulsion between peripheral phenyl groups of the DPP<sup>2-</sup> ligands and the coordinated POMs. The displacement of each atom of porphyrin macrocycles of **5**, **6**, and **7** is depicted in Figure S2 (Supporting Information), and those porphyrin macrocycles exhibit much smaller distortions compared with that of **1**.<sup>24</sup>

The direct coordination should be ascribed to strong Lewis acidity of the Mo(V) center in the non-planar DPP<sup>2-</sup> ligand:<sup>24</sup> a planar [Mo(TPP)(O)(H<sub>2</sub>O)]<sup>+</sup> does not react with POMs employed here to afford their direct coordination to form a discrete complex, in sharp contrast to the case of **1**. These results indicate that our strategy works successfully; the weakly bound aqua ligand in **1** can be replaced by negatively charged and more Lewis-basic POM ligands. Thus, the enhanced Lewis acidity of the [Mo(DPP)(O)]<sup>+</sup> unit gives rise to a strong coordination bond with the Keggin-type POM to access a new category of discrete molecular assemblies derived from ensembles of metalloporphyrins and POMs.

In spite of the feature that all *Porphyrin Hamburgers* are obtained as 2:1 complexes of metalloporphyrins and POM, each complex exhibits different bridging bond angles of Mo(1)–O(2)–W(1) (Figure 2). Especially, **5** and **7** involve two different coordination bond angles in one molecule, forming unsymmetrical molecular environments in the crystals (Table 1). The Mo=O bond lengths of the [Mo(DPP)(O)]<sup>+</sup> units in **5**, **6**, and **7** are 1.669(7) Å, 1.680(11) Å, and 1.682(8) Å (Mo(1)–O(1)), respectively.

**Table 1.** Bond Distances (Å) and Angles (deg) for **5**, **6**, and **7**

assignment	compound		
	<b>5</b> <sup>a</sup>	<b>6</b>	<b>7</b> <sup>a</sup>
Mo(1)–O(1)	1.669(7)	1.680(11)	1.682(8)
Mo(1)–O(2)	2.407(7)	2.261(11)	2.282(8)
W(1)–O(2)	1.686(7)	1.726(11)	1.713(8)
W(2)–O(2)	1.737(7)		1.791(9)
Mo(1)–O(2)–W(1)	167.3(4)	169.11(8)	171.7(6)
Mo(1)–O(2)–W(2)	149.3(4)		153.2(6)

<sup>a</sup> Structure refinements were made by using the “Squeeze” method.

The corresponding Mo–O bonds with the Keggin-type POM are 2.407(7) Å, 2.261(11) Å, and 2.282(8) Å (Mo(1)–O(2)), respectively. The two Mo(V) centers in these complexes seem to be in different coordination environments because of the difference in coordination bond angles. This difference is maintained even in solutions as observed by EPR measurements described below. The compound **5** includes the most distorted porphyrin macrocycle compared with other complexes in light of the displacement of each atom from the mean plane of 24 atoms in the porphyrin core (Figure S2 in Supporting Information). In addition, UV–vis spectral titration with base, elemental analysis, and an ESI-MS measurement to detect TBA<sup>+</sup> support that **7** has one proton and two of TBA<sup>+</sup> ion in its formula as a counteranion, despite that **5** and **6** include not TBA<sup>+</sup> but only protons as counteranions in their formulas. Details of these particular differences will be discussed below.

In the *ac* plane of these three crystals, intermolecular  $\pi$ – $\pi$  interactions are operating among peripheral phenyl groups to give rise to a two-dimensional (2D) sheet structure.<sup>26</sup> Though the peripheral phenyl groups of **5** and **7** are not in the eclipse conformation as in the crystal of **6** but in a slide form with an offset from each other, they also exhibit such  $\pi$ – $\pi$  interactions in the *ac* plane and give rise to the 2D sheets. Toward the direction of the crystallographic *b* axis, the sheets stack layer by layer through edge-to-face  $\pi$ – $\pi$  interactions among peripheral phenyl groups and CH $\cdots$ O hydrogen bonding between the phenyl C–H and the Mo=O moieties. The stacking of

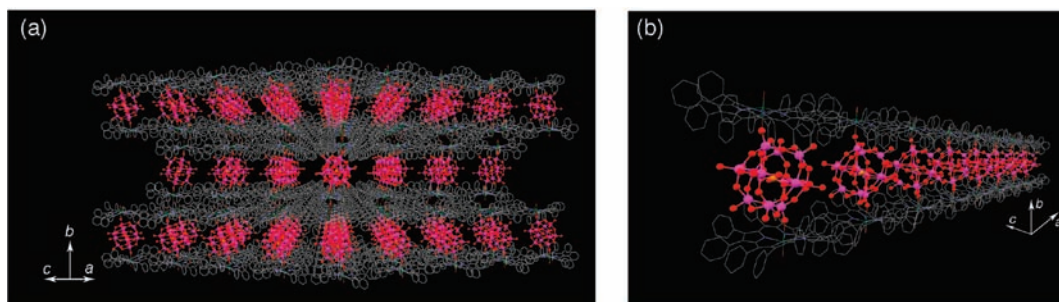


**Figure 3.** Three dimensional (a) and one-dimensional (b) descriptions of the crystal packing of **5**: the DPP<sup>2-</sup> ligand, wireframes; green, Mo; pink, W; red, O; orange, phosphorus.

the 2D sheets affords a layered structure in the crystal as shown in Figure 3a having two channels running into the directions of [1 0 0] and [0 0 1] in each crystal. Considerable amount of H<sub>2</sub>O and CH<sub>3</sub>CN molecules of crystallization was detected by TG-MS measurements for **6**, however, their severe disorder did not allow us to determine their positions in the channels. The crystals of **6** exhibited the thermodynamic stability up to about 300 °C, supporting its robustness as a solid material.<sup>26</sup> Besides the detection of H<sub>2</sub>O and CH<sub>3</sub>CN as solvent molecules of crystallization, we could not determine the positions of those solvent molecules in X-ray crystallography because of their severe disorder. AcOEt and hexane, which were used as solvents for the recrystallization, were not detected in the TG-MS analysis. Along the direction of the crystallographic *a* axis, as depicted in Figure 3b, a one-dimensional (1D) array of the *Porphyrin Hamburgers* can be observed by virtue of intermolecular  $\pi$ - $\pi$  interactions among peripheral phenyl groups like gear wheels (see Scheme 1).

XPS (X-ray photoelectron spectroscopy) measurements of **1**, **3**, and **6** in the solid state were carried out to clarify the oxidation states of metal ions in the *Porphyrin Hamburger* (Supporting Information, Figure S3). The aqua complex **1** showed two peaks at 235.3 and 232.4 eV and the complex **6** at 235.5 and 232.4 eV for binding energies, respectively, which were assigned to 3d<sub>3/2</sub> and 3d<sub>5/2</sub> of molybdenum.<sup>34</sup> The result allowed us to confirm that the Mo ions in **6** were in the Mo<sup>V</sup> oxidation state as well as in **1**. As for the tungsten ion in the POM, **3** and **6** exhibited peaks assigned to W 4f<sub>5/2</sub> and W 4f<sub>7/2</sub> at 36.72 and 34.51 eV for **3**, and 37.13 and 34.90 eV for **6**, respectively. Thus, the W ions in **6** were all intact to be in the W<sup>VI</sup> oxidation state as in the case of **3**.<sup>35</sup> These results indicate that no redox reactions occur in the course of the formation of the *Porphyrin Hamburger*.<sup>26</sup> On the basis of these results, the Mo and W ions in **5** and **7** should be in the same oxidation states as those in **6**. In the light of both the oxidation states of metal ions involved and no observation of TBA<sup>+</sup> as counter cations for the negatively charged POMs in X-ray analysis, it is reasonable to assume that the POM moiety in *Porphyrin Hamburger* should be protonated to achieve the charge balances.

Protonation of POM has been reported to occur at the terminal oxo groups with H<sub>5</sub>O<sub>2</sub><sup>+</sup> for hydrated species<sup>36</sup> and at the  $\mu$ -oxo moieties for dehydrated ones.<sup>37</sup> Although the position and the situation of the protonation are not clear for **5**–**7**, their protonation has been proven by spectroscopic titration with bases in solution as described below.

**Protonated Heteropolyoxometalates.** To clarify the protonation of the POM moieties in the *Porphyrin Hamburgers* for charge balance, spectroscopic titration was performed by using NEt<sub>3</sub> a base in CH<sub>2</sub>Cl<sub>2</sub> and PhCN. In the UV–vis spectroscopic titration, we could observe spectral change upon addition of NEt<sub>3</sub> into the solution of **5** in PhCN up to about 1 equiv, and no further change was observed for adding more than about 1 equiv of the base (see Figure S4(a) and (b) in Supporting Information). The change of absorbance was monitored at 484.5 nm for **5** in accordance with the addition of NEt<sub>3</sub>, and the change ceased after addition of 1 equiv of the base. In the case of **6**, its absorption spectrum in CH<sub>2</sub>Cl<sub>2</sub> exhibited slight change upon addition of NEt<sub>3</sub> with three isosbestic points at 510, 556, and 635 nm. The change of absorbance at 635 nm was monitored and it stopped after the addition of 2 equiv of NEt<sub>3</sub> (see Figure S4 (c) and (d) in the Supporting Information).

In the course of spectroscopic titration of **7** in CH<sub>2</sub>Cl<sub>2</sub>, the spectral change was observed as shown in Figure 4a with isosbestic points at 493, 509, 552, and 575 nm. The spectral change ceased at the addition of 1 equiv of NEt<sub>3</sub>, and no apparent change was observed by further addition of the base as depicted in Figure 4b. A stronger base (proton sponge) was used for **7** under the same conditions: However, the spectral change was also stopped at the addition of 1 equiv of the proton sponge. These results clearly indicate that **7** bears only one proton in its formula. Together with the results of elemental analysis and MALDI-TOF-MS measurements (see the next section), the molecular formula of **7** is determined to be (TBA)<sub>2</sub>[{Mo(DPP)(O)}<sub>2</sub>(HBW<sub>12</sub>O<sub>40</sub>)].<sup>38</sup>

These observations lend credence to the existence of protons in the POM moieties in the *Porphyrin Hamburgers*. Since the number of [Mo(DPP)(O)]<sup>+</sup> units which can

(34) Arul Dhas, N.; Gedanken, A. *J. Phys. Chem. B* **1997**, *101*, 9495.

(35) (a) Liu, J.; Wang, W.; Wang, G.; Zhao, B.; Sun, S. *Polyhedron* **1994**, *13*, 1057. (b) Wang, Y.; Guo, C.; Chen, Y.; Hu, C.; Yu, W. *J. Colloid Interface Sci.* **2003**, *264*, 176.

(36) Brown, G. M.; Noe-Spirlet, M.-R.; Busing, W. R.; Levy, H. A. *Acta Crystallogr.* **1977**, *B33*, 1038.

(37) Lee, K. L.; Mizuno, M.; Okuhara, T.; Misono, M. *Bull. Chem. Soc. Jpn.* **1989**, *62*, 1731.

(38) ESI-MS measurements (positive mode) of **7** in CH<sub>3</sub>OH/CH<sub>2</sub>Cl<sub>2</sub> allowed us to observe a peak cluster assigned to TBA<sup>+</sup> (calcd: *m/z* = 242.47) at *m/z* = 242.31 to confirm its existence as a countercation. In the X-ray measurement, however, the involvement of TBA<sup>+</sup> ions was not clarified because of their severe disorder.

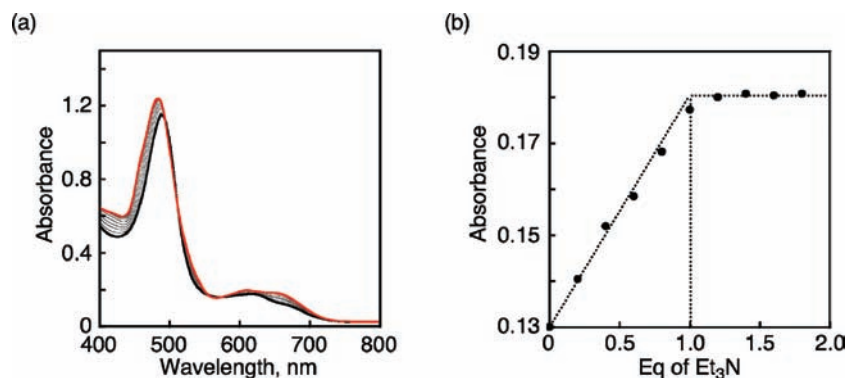


**Figure 4.** (a) UV-vis spectral changes of **7** ( $1.0 \times 10^{-5}$  M) upon addition of  $\text{NEt}_3$  (1 mM). (b) Changes of absorbance at 658 nm upon addition of  $\text{NEt}_3$ .

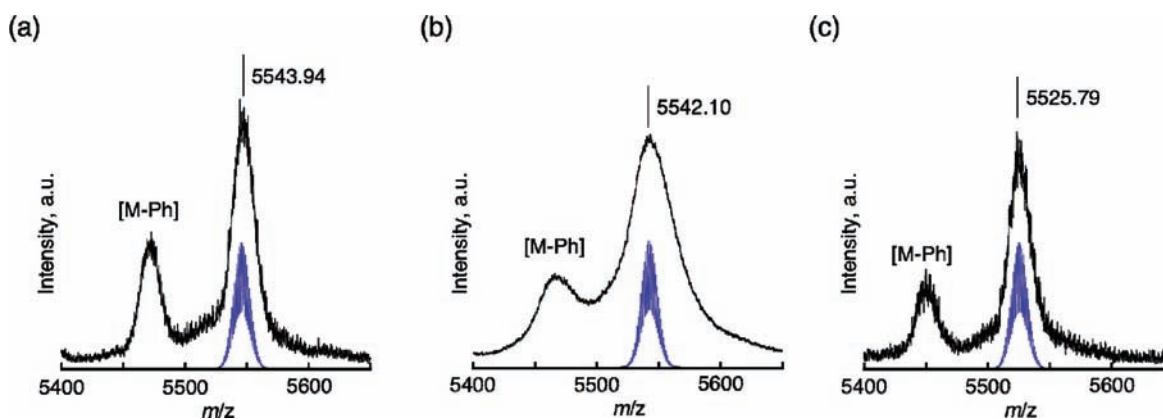


**Figure 5.** MALDI-TOF-MS spectra (negative mode; black) and computer simulations (blue) of **5** (a), **6** (b), and **7** (c). The measurements were made in  $\text{CH}_2\text{Cl}_2$  (matrix;  $\alpha$ -cyano-4-hydroxy-cinnamic acid (CHCA)).

bind to a Keggin-type POM should be limited to two because of steric requirements, the residual negative charge of the POM moiety is canceled by the protonation, probably depending on its Lewis basicity. Further requirement for positive charge in **7** is made by the external counter cations such as  $\text{TBA}^+$ , as demonstrated by its elemental analysis, to achieve the charge balance.

It should be noted that the POM in the *Porphyrin Hamburger* is protonated even under neutral conditions, besides the fact that a POM is an extremely stronger Brønsted acid in  $\text{H}_2\text{O}$  than  $\text{H}_2\text{SO}_4$  and  $\text{HNO}_3$ .<sup>39</sup> It is probably due to the lower polarity of the solvents ( $\text{CH}_2\text{Cl}_2$ ,  $\text{AcOEt}$ ,  $\text{CH}_3\text{CN}$ , and hexane) used than that of  $\text{H}_2\text{O}$  and the less polar environment formed by the two highly hydrophobic  $\text{DPP}^{2-}$  ligands. Although a determinant of the number of protonations is unclear at this stage, the *Porphyrin Hamburger* surely involves the unique protonation of the POM moiety in a specific environment formed by the two directly bound  $[\text{Mo}(\text{DPP})(\text{O})]^+$  units.

**Stability of *Porphyrin Hamburger* in Solution.** MALDI-TOF-MS spectra of *Porphyrin Hamburgers* (**5**, **6**, and **7**) in  $\text{CH}_2\text{Cl}_2$  (negative mode) are shown in Figure 5. CHCA ( $\alpha$ -cyano-4-hydroxycinnamic acid) was used as a matrix.<sup>40</sup> Under such conditions, they exhibited peak clusters at

5543.94 (**5**) and 5542.10 (**6**), which agree with the calculated mass numbers of monodeprotonated molecular monoanions ( $[\text{M} - \text{H}]^-$ ). A peak cluster was detected at 5525.79, assignable to a monoprotonated molecular ion ( $[\text{M} + \text{H}]^+$ ) of the anion part of **7**,  $[\{\text{Mo}(\text{DPP})(\text{O})\}_2(\text{H}_2\text{BW}_{12}\text{O}_{40})]^-$ . Although the isotopic patterns are unclear in the observed spectra, these results indicate that the *Porphyrin Hamburgers* maintain their structures even in solutions as in the solid state and allow us to treat them in solution as discrete molecular entities.

**Electrochemical Measurements.** We investigated redox behaviors of *Porphyrin Hamburgers* in PhCN solution at room temperature in the presence of  $\text{TBAPF}_6$  (0.1 M). All the redox potentials are summarized in Table 2. In cyclic voltammetric measurements, reversible redox waves were observed for **1–7**. Those cyclic voltammograms (CVs) and differential plus voltammograms (DPVs) of **1** to **7** are shown in Figure 6 (**5–7**) and Figure S5 in Supporting Information (**1**, **2–4**). The reversible multiple-redox waves observed in CVs also lend credence to the stability and robustness of the *Porphyrin Hamburgers* even in PhCN. In comparison of the voltammograms of the *Porphyrin Hamburgers* with those of the precursor (**1**, Supporting Information, Figure S5), redox waves for **5**, **6**, and **7** observed at 1.29, 1.26, and 1.16 V were assigned to one-electron oxidation of the  $\text{DPP}^{2-}$  ligand of **5**, **6**, and **7**, respectively.<sup>41</sup> The values for **5** and **6** are similar to that of **1**; however, that for **7** is negatively shifted from that of **1** ( $\Delta E_{1/2} = -0.12$  V). The redox processes observed at 0.06 V,

(39) (a) Izumi, Y.; Matsuo, K.; Urabe, K. *J. Mol. Catal.* **1983**, *18*, 299. (b) Misono, M. *Chem. Rev.* **1987**, *29*, 269. **1988**, *30*, 339. (c) Okuhara, T.; Nishimura, T.; Watanabe, H.; Misono, M. *J. Mol. Catal.* **1992**, *74*, 247.

(40) The use of other matrixes resulted in no observation of peak clusters assignable to negative ions derived from the conglomerates.

Table 2. Redox Potentials of 1 to 7 in PhCN<sup>a</sup>

compound	E vs SCE, V						
	Mo <sup>IV</sup> /Mo <sup>V</sup> ( $\Delta E$ ) <sup>d</sup>	Por <sup>2-</sup> /Por <sup>-b</sup> ( $\Delta E$ )	Por <sup>3-</sup> /Por <sup>2-</sup> ( $\Delta E$ )	Por <sup>4-</sup> /Por <sup>3-</sup> ( $\Delta E$ )	POM <sup>4-</sup> /POM <sup>3-</sup> <sup>c</sup> ( $\Delta E$ )	POM <sup>5-</sup> /POM <sup>4-</sup> ( $\Delta E$ )	POM <sup>5-</sup> /POM <sup>6-</sup> ( $\Delta E$ )
1	0.03 (0.07)	1.28 (0.08)	-1.03 (0.07)	-1.42 (0.08)			
2					-0.49 (0.13)	-1.04 (0.21)	
3						-0.97 (0.16)	-1.51 (0.14)
4							-1.52 (0.14)
5	0.06 (0.09)	1.29 (0.10)	-1.12 (0.10)	-1.47 (0.10)	-0.31 (0.06)	-0.82 (0.08)	
6	0.00 (0.06)	1.26 (0.09)	-1.04 (0.06)	-1.41 (0.08)		-0.87 (0.09)	
7	-0.10 (0.08)	1.16 (0.10)	-1.12 (0.09)	(-1.49) <sup>e</sup> (0.12)			(-1.49) <sup>e</sup> (0.12)

<sup>a</sup> At room temperature under Ar; 0.1 M TBAPF<sub>6</sub> as an electrolyte. <sup>b</sup> Por<sup>n-</sup>: DPP<sup>2-</sup> ligand. <sup>c</sup> POM<sup>n-</sup>: Keggin-type heteropolyoxometalate. <sup>d</sup>  $\Delta E = E_{\text{ox}} - E_{\text{red}}$  (V). <sup>e</sup> Overlapped.

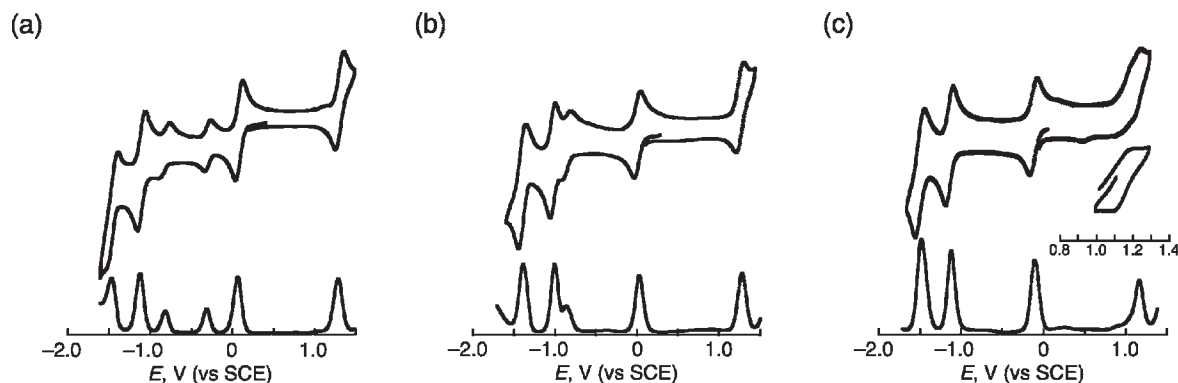


Figure 6. Cyclic voltammograms (CV) and differential plus voltammograms (DPV) for 5 (a), 6 (b), and 7 (c) in PhCN, at room temperature under Ar in the presence of 0.1 M TBAPF<sub>6</sub>.

0.00 V, -0.10 V in 5, 6, and 7 were ascribed to the Mo<sup>V</sup>/Mo<sup>IV</sup> redox couples of 5, 6, and 7, respectively.<sup>42</sup> These values are similar to that for 1, and the peak separation of the redox waves are almost intact upon coordination of POMs. The first and second one-electron reduction processes of the DPP<sup>2-</sup> ligand were observed at -1.12 and -1.47 V for 5, -1.04 and -1.41 V for 6, and -1.12 and -1.49 V<sup>43</sup> for 7, respectively.<sup>41</sup> Those values were also similar to those of 1 (-1.03 and -1.42 V, respectively). Concerning the second reduction of the DPP<sup>2-</sup> ligand in 7, its redox wave is assumed to be overlapped with that of the first reduction of [HBW<sub>12</sub>O<sub>40</sub>]<sup>4-</sup>: the peak separation (0.12 V) is larger than that of 1 (0.08 V) and those of POMs in 5 (0.06 and 0.08 V) and 6 (0.09 V). Reversible redox waves observed at -0.82 and -0.31 V for 5 and at -0.87 V for 6 exhibited half of the peak currents as compared to those of other redox waves derived from the [Mo(DPP)(O)]<sup>+</sup> units. Therefore, we assigned those redox waves to the two-electron and one-electron reduction processes of the trapped [HPW<sub>12</sub>O<sub>40</sub>]<sup>2-</sup> moiety and one-electron reduction of the trapped [H<sub>2</sub>SiW<sub>12</sub>O<sub>40</sub>]<sup>2-</sup> moiety, respectively, by comparing with those of precursors (2 and 3, respectively). In the CVs of 6 and 7, their

second one-electron reduction processes were not observed. In addition, the first one-electron reduction process of [HBW<sub>12</sub>O<sub>40</sub>]<sup>4-</sup> is assumed to be overlapped with the second one-electron reduction of DPP<sup>2-</sup> ligand (*vide supra*).

The shifts of the redox potentials seem to be small; however, they should stem from a sum of results from the change of the porphyrin distortion caused by coordination of POM, coordination strength of POM to the [Mo(DPP)(O)]<sup>+</sup> unit, difference in solvation, and so on. Even though the shifts are small, the *Porphyrin Hamburgers* exhibit clear and reversible redox processes at different potentials as compared to those of components, indicating their stability in solution.

**EPR Measurements.** EPR spectra of 5, 6, and 7 in CH<sub>2</sub>Cl<sub>2</sub> provide clear and strong evidence to support the persistence of *Porphyrin Hamburgers* in solution. In EPR measurements in CH<sub>2</sub>Cl<sub>2</sub> at room temperature, each *Porphyrin Hamburger* showed a different EPR spectrum as shown in Figure 7. Each  $A_N$  value was estimated by computer simulations using a WinSimESR simulation program.<sup>44</sup> The EPR parameters obtained are summarized in Table 3. The precursor of the complex, [Mo(DPP)(O)(H<sub>2</sub>O)]ClO<sub>4</sub>(1), showed a clear and well-resolved EPR signal assigned to the Mo(V) center ( $I = 0$ ) at  $g = 1.964$  showing superhyperfine coupling ( $A_N = 2.15$  G) because of the nuclear spins of the four nitrogen atoms in the porphyrin ligand. However, this superhyperfine coupling constant is smaller than that of planar [Mo<sup>V</sup>(TPP)(O)(OCH<sub>3</sub>)] ( $A_N = 2.5$  G).<sup>45</sup> This indicates that 1 has more weakened interactions between the lone

(41) (a) Guillard, R.; Perić, K.; Barbe, J.-M.; Nurco, D. J.; Smith, K. M.; Caemelbecke, E. V.; Kadish, K. M. *Inorg. Chem.* **1998**, *37*, 973. (b) Kadish, K. M.; Caemelbecke, E. V.; D'Souza, F.; Lin, M.; Nurco, D. J.; Medforth, C. J.; Forsyth, T. P.; Krattinger, B.; Smith, K. M.; Fukuzumi, S.; Nakanishi, I.; Shelnutt, J. A. *Inorg. Chem.* **1999**, *38*, 2188.

(42) Malinski, T.; Hanley, P. M.; Kadish, K. M. *Inorg. Chem.* **1986**, *25*, 3229.

(43) This redox wave is assumed to be an overlapped one including those derived from the redox processes of Por<sup>4-</sup>/Por<sup>3-</sup> and POM<sup>5-</sup>/POM<sup>6-</sup>, judging from a large peak separation of the redox couple ( $\Delta E = 0.12$  V).

(44) (a) Duling, D. R.; Motten, A. G.; Mason, R. P. *J. Magn. Reson.* **1988**, *77*, 504. (b) Duling, D. R. *J. Magn. Reson.* **1994**, *104*, 105.



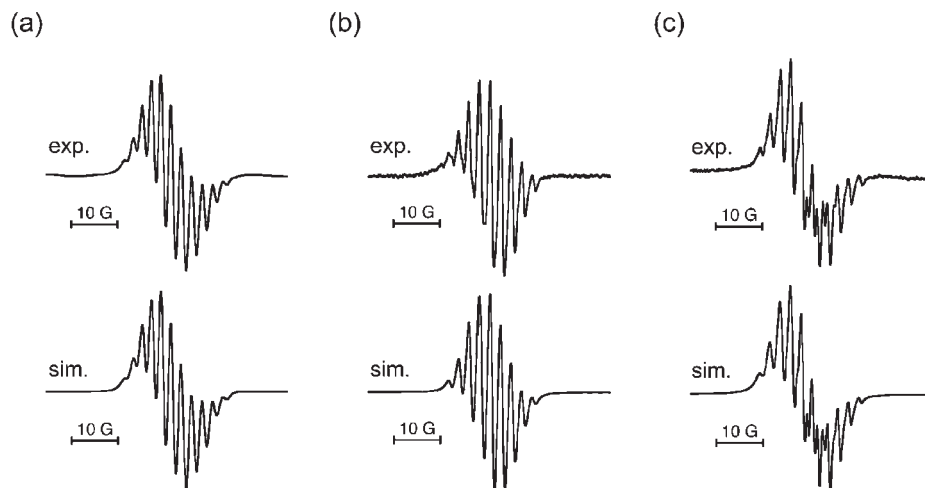


**Figure 7.** EPR spectra of **5** (a), **6** (b), and **7** (c) for the Mo<sup>V</sup> ( $S = 1/2$ ,  $I = 0$ ) signal in CH<sub>2</sub>Cl<sub>2</sub> at room temperature: Frequency, 9.454 GHz (a), 9.457 GHz (b), 9.113 GHz (c); Power, 1.0 mW; Modulation; 100.00 kHz, 0.1 G.

**Table 3.**  $g$  and  $A_N$  (G) Values of **1**, **5**, **6**, and **7** in CH<sub>2</sub>Cl<sub>2</sub> at Room Temperature

compound	$g$	$A_N$
<b>1</b>	1.964	2.15
<b>5</b>	1.965	2.03
	1.962	1.90
<b>6</b>	1.963	2.20
<b>7</b>	1.965	2.16
	1.966	2.14

pairs of pyrroles of the DPP<sup>2-</sup> ligand and the  $d_{x^2-y^2}$  orbital of the Mo(V) center, compared to that of the planar Mo(V)-porphyrin complex. The weaker interaction of DPP<sup>2-</sup> with the Mo(V) center in **1** also supports its higher Lewis acidity than that of the planar counterpart. This strong Lewis acidity of the Mo(V) center in **1** should result in the direct coordination of the Keggin ligand.

The EPR signal of **6** assigned to the Mo(V) center ( $I = 0$ ) was observed at  $g = 1.963$  with superhyperfine coupling ( $A_N = 2.20$  G) with four nitrogen nuclei in the DPP<sup>2-</sup> ligand. The complexes of **5** and **7** exhibiting two different coordination bond angles between the Mo<sup>V</sup> centers and the corresponding POMs showed dissymmetric EPR spectra (Figure 7a,c). Computational simulations of those spectra gave two different  $g$  and  $A_N$  values for overlapped signals. This indicates that two nonequivalent molybdenum atoms are involved in **5** and **7** in the solution, consistent with the structures observed in their crystal structures in which the two Mo<sup>V</sup> centers are in the different coordination environments. The  $A_N$  values of complexes are smaller than that of the planar Mo(V)-porphyrin and comparable to that of the precursor (Table 3), reflecting the non-planarity of the DPP ligand in *Porphyrin Hamburgers* as observed in the crystal structures.

## Summary

We established a synthetic methodology for the construction of covalently linked molecular metalloporphyr-

in-heteropolyoxometalate complexes, named *Porphyrin Hamburgers*. *Porphyrin Hamburgers* can be synthesized as nanosized molecules by employing three types of Keggin-type POMs and have been crystallographically characterized as 2:1 complexes of the Mo(V)-DPP complex and protonated Keggin-type POMs employed. As for a metalloporphyrin unit, enhanced Lewis acidity of the metal center coordinated by the DPP<sup>2-</sup> ligand plays an indispensable role to hold Lewis-basic Keggin-type POMs in the coordination sphere of the Mo<sup>V</sup>(DPP) unit to stabilize the complexes even in solution. In these complexes, the existence of protons in the POM moiety may provide the structural differences in terms of the bond angles of the Mo–O–W linkage and may alter the molecular symmetry not only in the solid state but also in solutions. In addition, those complexes maintain their structures even in solution as well as in the solid state and showed reversible multiple-redox processes and EPR spectra, reflecting the crystal structures. The stability may allow us to expect new functionality of those complexes involving catalysis in solution and to encounter novel supramolecular assemblies in combination with other hydrogen-bonding guest molecules.

**Acknowledgment.** We are grateful to financial support provided by Grants-in-Aids (Nos. 20108010 and 21111501) and a Global COE program, “the Global Education and Research Center for Bio-Environmental Chemistry” from the Japan Society of Promotion of Science (JSPS), a JSPS predoctoral fellowship (20-00804 to A.Y.), and by KOSEF/MEST through WCU project (R31-2008-10010-0). We also appreciate Dr. Sayaka Uchida (The University of Tokyo) for her helpful advice on the synthesis of POMs.

**Supporting Information Available:** Details of crystallographic analysis, crystallographic parameters, ORTEP drawings of **1**, displacements of atoms in porphyrin cores for **5–7**, XPS spectra of **1**, **3**, and **6**, CV and DPV traces of **1–4**, and crystallographic data of **5–7** (cif format). This material is available free of charge via the Internet at <http://pubs.acs.org>.

(45) Ledon, H. J.; Bonnet, M. C.; Brigandat, Y.; Varescon, F. *Inorg. Chem.* **1980**, *19*, 3488.